Polymer 50 (2009) 5685–5692

Contents lists available at ScienceDirect

Polymer

journal homepage: www.elsevier.com/locate/polymer

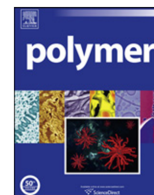

An approach to develop high-Tg epoxy resins for halogen-free copper clad laminates

Hong Tze Lin [a], Ching Hsuan Lin [a,*], Yu Ming Hu [a], Wen Chiung Su [b]

[a] Department of Chemical Engineering, National Chung Hsing University, Taichung 402, Taiwan
[b] Chung Shan Institute of Science and Technology, Lungtan, Tauyuan, Taiwan

A R T I C L E I N F O

Article history:
Received 2 June 2009
Received in revised form
1 September 2009
Accepted 30 September 2009
Available online 2 October 2009

Keywords:
Phosphorus
Epoxy
Flame retardant

A B S T R A C T

A series of advanced epoxy resins **(2)** were prepared by the nucleophilic addition of cresol novolac epoxy (CNE) with a benzoxazine monomer **(1)**, which is prepared by a one-pot procedure using 2-hydroxybenzaldehyde, 4-aminophenol and 9, 10-dihydro-9-oxa-10-phosphaphenanthrene 10-oxide **(DOPO)** as starting materials. The nucleophilic addition was monitored by epoxy equivalent weight titration and NMR analysis. Based on this approach, the overall number of functionality of the resulting epoxy resins was retained because a curable benzoxazine linkage was also incorporated after the nucleophilic addition. As a result, high-Tg thermosets qualified for the UL-94 V-0 rating can be achieved after curing. When an UL-94 V-0 rating was achieved, Tg as high as 245 °C (DMA data) was obtained for 4,4′-diaminediphenyl sulfone (DDS)-cured systems. The corresponding phosphorus content for the UL-94 V-0 rating was as low as 0.61 wt%. The flame-retardant nature of oxazine linkage and nitrogen–phosphorus synergistic effect might be responsible for the low phosphorus content required for flame retardancy.

© 2009 Elsevier Ltd. All rights reserved.

1. Introduction

Advanced epoxy resins, which are usually prepared by the reaction of epoxy resins and biphenols in the catalysis of triphenylphosphine or imidazole, have been widely used in the electrical laminates for printed circuit board [1–7]. Among the advanced epoxy resins, the brominated epoxy resins, which results from the advancement of diglycidyl ether of bisphenol A and the tetrabromobisphenol A, are widely useful for FR-4 copper clad laminates [8]. However, they may release hydrogen bromide, dibenzo-p-dioxin and dibenzofuran during combustion, causing corrosion and toxicity [8].

In addition to the halogen-based compound, alkyne-based [9–11], phosphorus-based [1–6,12–17] and deoxybenzoin-based [18–20] compounds, which can retard the combustion of polymers by covering the outer layer of the plastic with a nonflammable coating, are other alternatives for flame retardancy. Several years ago, Komori et al. [1], Nakamura et al. [2], Takahashi et al. [3,4], Yoshizawa et al. [5], and Wang et al. [6] reported the synthesis of phosphorus-based difunctional advanced epoxy resins for halogen-free copper clad laminate. Although the resins displayed good flame retardancy, they resulted in low Tg after curing. The high epoxy equivalent weight of the resulting epoxy resulted in low crosslinking density, and leaded to low glass transition temperature. In our previous paper [12], we reported the **DOPO**-modified epoxy resins by nucleophilic addition of **DOPO** on CNE. Based on the resins and their derivatives, medium to high-Tg halogen-free copper clad laminates were produced and commercialized [21]. In that paper, the phosphorus element was introduced via the nucleophilic addition of DOPO on the oxirane of CNE. As a result, the overall number of functionality of the resulting epoxy resins decreased significantly with the content of DOPO, leading to thermosets with an obvious decrease in Tg with the phosphorus content. The significant reduction in Tg with the phosphorus content was also observed by Qi et al. [22], and Döring et al. [23,24]. Recently, Döring et al. reported the synthesis of flame-retardant epoxy resins without significant reduction in Tg by reacting a difunctional compound ($DOPO_2$-TDA) with CNE [25]. However, from an industry viewpoint, reacting a multi-functional epoxy resin with a difunctional compound may lead to gel if the reaction is not controlled well [26]. Besides, the significant increase in the molecular weight may result in high viscosity, limiting its solubility and reducing its processibility.

Besides epoxy resins, benzoxazines are another kind of curable resins that can be polymerized to thermosets [20–24]. In this paper, by combining the chemistry of epoxy and benzoxazine, we report a method of preparing multi-functional epoxy resins without decreasing the overall number of functionality. Herein, a phosphorus-containing benzoxazine **(1)** with a hydroxyl linkage was designed. Based on **(1)**, a series of advanced epoxy resins **(2)** with

* Corresponding author.
E-mail address: linch@nchu.edu.tw (C.H. Lin).

0032-3861/$ – see front matter © 2009 Elsevier Ltd. All rights reserved.
doi:10.1016/j.polymer.2009.09.075

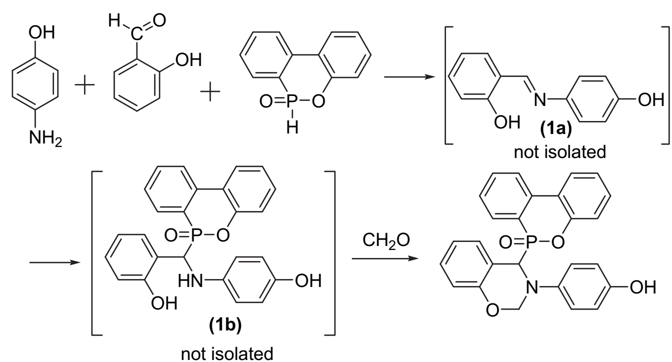

Scheme 1. One-pot synthesis of benzoxazines (**1**).

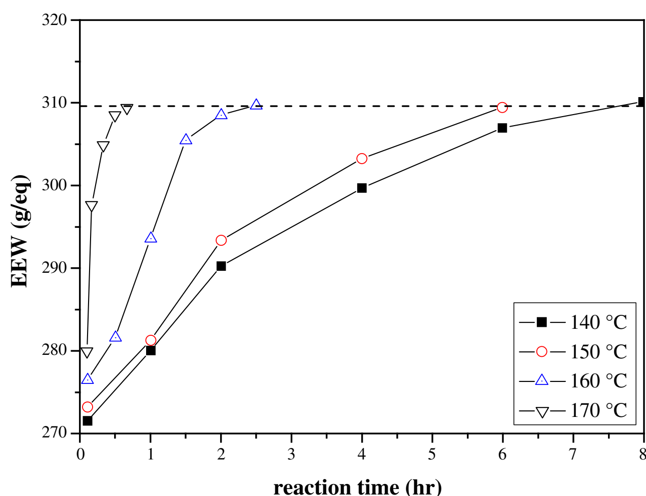

Fig. 1. The plot of EEW versus reaction time at various reaction temperatures for (**2–1.5**).

various phosphorus contents were prepared by the nucleophilic addition phenolic OH of **(1)** on the oxirane of CNE. Although the number of functionality of oxirane was reduced after the nucleophilic addition, the overall number of functionality of the resulting resins was not reduced because a curable benzoxazine linkage was also incorporated after the addition. That is, the overall number of functionality was maintained after incorporating the phosphorus element. As a result, flame retardant thermosets with high Tg can be expected. Besides, the effect of reaction conditions on the preparation of **(2)** was monitored by EEW titration and NMR analysis. After curing **(2)** with 4,4′-diaminediphenyl sulfone (DDS) and dicyanodiamine (DICY), the thermal properties, dimensional stability and flame retardancy of the resulting epoxy thermosets were evaluated.

2. Experimental section

2.1. Materials

9,10-Dihydro-9-oxa-10-phosphaphenanthrene 10-oxide (DOPO) was purchased from TCI. 2-Hydroxybenzaldehyde was purchased from Showa. Cresol novolac epoxy resin (CNE) with epoxy equivalent weight of 200 g/eq was kindly supplied by Chang Chun Plastics, Taiwan in the trade name of ELD-200. 4-Aminophenol, 4,4′-diaminodiphenyl sulfone (DDS) and dicyandiamide (DICY) were purchased from Acros. N,N-dimethyl formamide (DMF) and tetrahydrofuran (THF) were purchased from Tedia and purified by distillation under reduced pressure over calcium hydride (Acros) and stored over molecular sieves. The other solvents used are commercial products and used without further purification.

2.1.1. Preparation of (1)

4-Aminophenol 6.55 g (0.06 mol), 2-hydroxybenzaldehyde 7.33 g (0.06 mol), DOPO 12.97 g (0.06 mol) and 150 mL methanol were introduced into a round-bottom 250 mL glass flask equipped with a nitrogen inlet, a condenser, and a magnetic stirrer (Scheme 1). The reaction mixture was stirred at room temperature for 12 h. Then, 4.92 g (0.06 mol) of 37% formaldehyde was added. The mixture was stirred at room temperature for 6 h, and then further stirred at reflux temperature for 12 h. After that, the solution was poured into water. The precipitate was filtered and dried at 80 °C in a vacuum oven. White powder (24.1 g, 91% yield) with two melting points of 230 and 237 °C (DSC) and an exothermic peak temperature of 241 °C was obtained. Since the phosphorus and the adjacent aliphatic carbon are

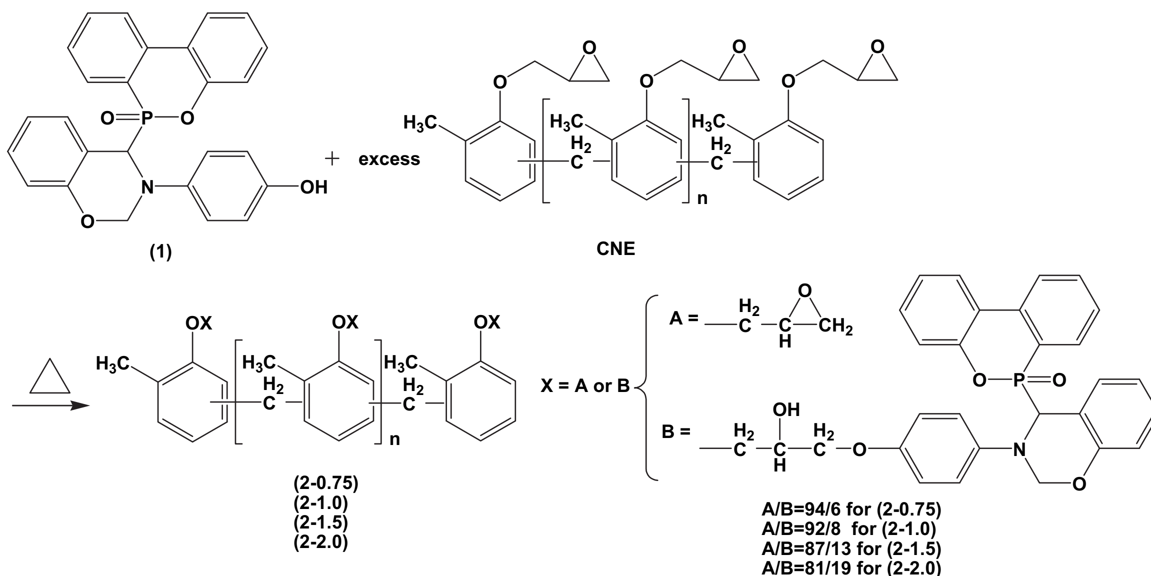

Scheme 2. Synthesis of advanced epoxy resins (**2**).

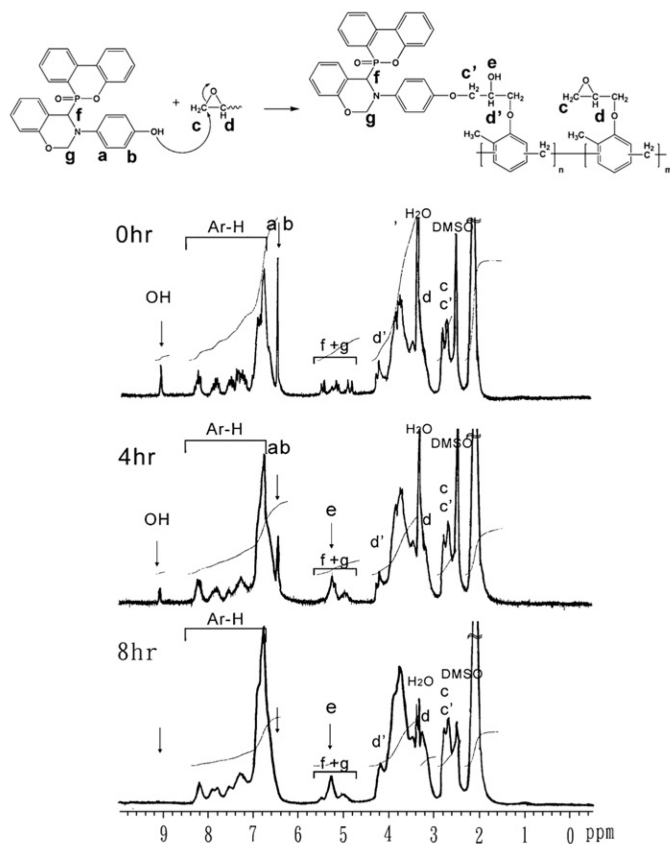

Fig. 2. The ^{1}H-NMR trace of **(2–1.5)** at 140 °C for various reaction times.

both chiral centers, two diastereomers exist in **(1)**. ^{1}H-NMR (ppm, DMSO-D$_6$), $\delta = 4.75$–5.39(H^5, $H^{5\prime}$, H^{24}, $H^{24\prime}$), 6.35–6.41(H^2, $H^{2\prime}$, H^3, $H^{3\prime}$), 6.74–6.79(H^8, $H^{8\prime}$, H^{10}), 6.90($H^{10\prime}$), 7.00(H^{11}), 7.08–7.12 (H^9, $H^{9\prime}$), 7.12–7.29($H^{11\prime}$, H^{13}, $H^{13\prime}$, H^{15}, $H^{15\prime}$), 7.32(H^{14}), 7.41($H^{14\prime}$), 7.48–7.52 (H^{21}, $H^{21\prime}$), 7.71–7.76(H^{20}, $H^{20\prime}$), 7.80–7.87(H^{22}, $H^{22\prime}$), 8.11(H^{16}), 8.13($H^{16\prime}$), 8.20(H^{19}), 8.22($H^{19\prime}$), 9.00(OH). HR-MS (FAB) *m*/*z*: calcd. for $C_{26}H_{20}O_4NP$ 441.11; anal., 442.11 for $C_{26}H_{20}O_4NP$ ($M + 1^+$).

2.1.2. *Preparation of epoxy resins (2)*

A typical preparation example for **(2–1.0)** (with phosphorus content of 1.0 wt%) is shown below, and the reaction equation is shown in Scheme 2. CNE 10 g was introduced into a 100 mL round glass flask equipped with a nitrogen inlet, a condenser, and a magnetic stirrer. After reaching the temperature to 160 °C, **(1)** 1.66 g was added. The mixture was stirred at that temperature for 2.5 h to obtain a light orange resin with EEW 268 g/eq (252 g/eq theoretically). **(2–0.75)** (with phosphorus content of 0.75 wt%) was synthesized in the same manner as described above using 1.2 g of **(1).** A light orange resin with EEW 258 g/eq was obtained (237 g/eq theoretically). **(2–1.5)** (with phosphorus content of 1.5 wt%) was synthesized in the same manner as described above using 2.71 g of **(1)**. A brown resin with EEW 309 g/eq was obtained (290 g/eq theoretically). **(2–2.0)** (with phosphorus content of 2.0 wt%) was synthesized in the same manner as described above using 3.98 g of **(1)**. A brown resin with EEW 366 g/eq was obtained (341 g/eq theoretically).

2.2. *Curing procedure*

Epoxy resins **(2)** were cured with two common curing agents for printed circuit boards, DDS and DICY, respectively. The reactant compositions were mixed in a 1:1 equivalent ratio. The mixture was crushed into fine powder and then heated on a hot plate at about 150 °C with continuous stirring until a homogeneous solution was obtained. The mixtures were cured at 180 °C, 200 °C, and 220 °C for 2 h, respectively. The samples were then allowed to cool slowly to room temperature to prevent cracking.

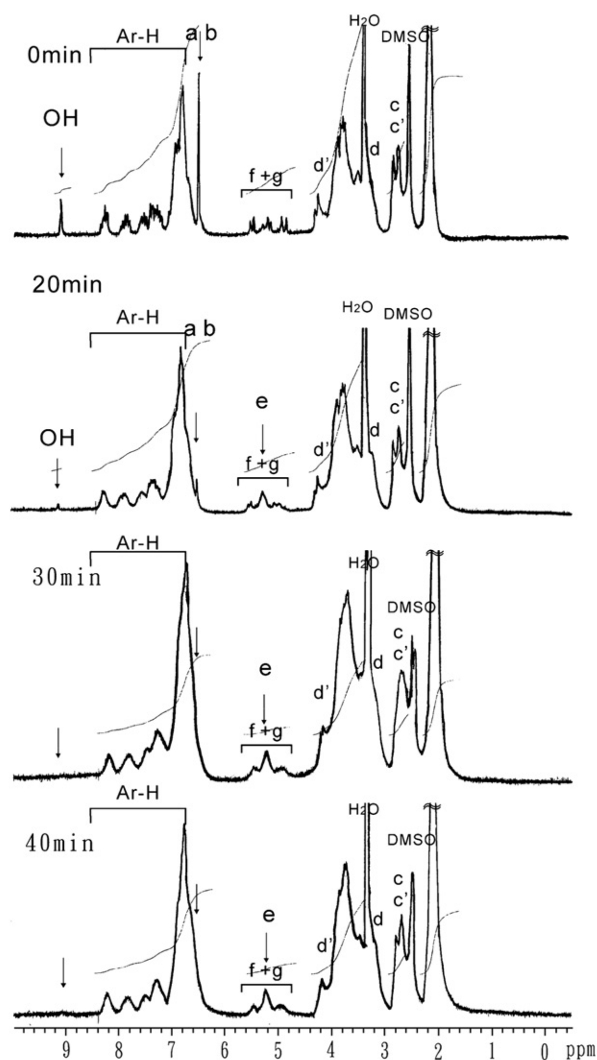

Fig. 3. The ^{1}H-NMR trace of **(2–1.5)** at 170 °C for various reaction times.

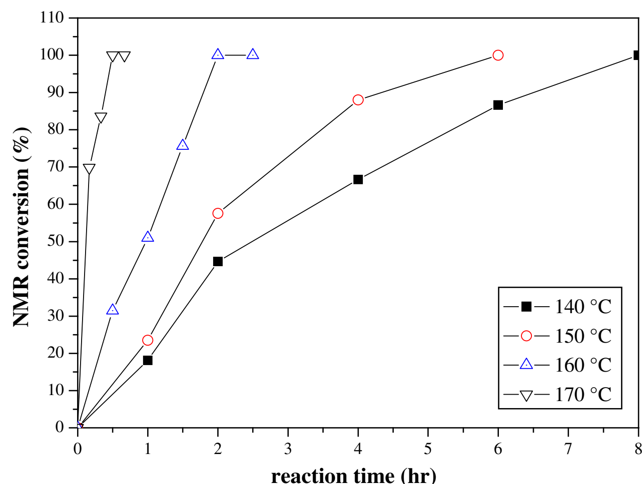

Fig. 4. The plot of conversion (based on NMR spectra) versus reaction time at various temperatures for **(2–1.5)**.

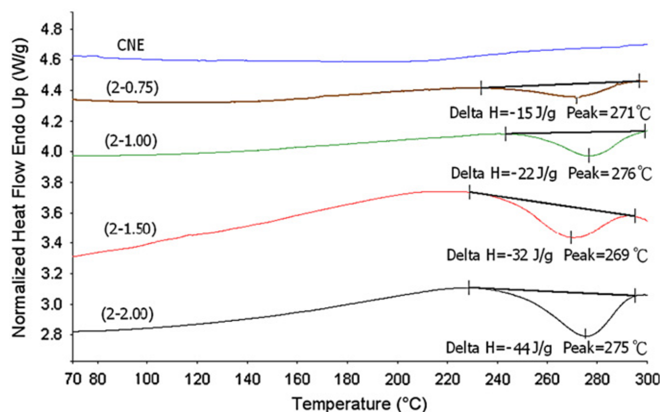

Fig. 5. DSC thermograms of CNE and **(2)**.

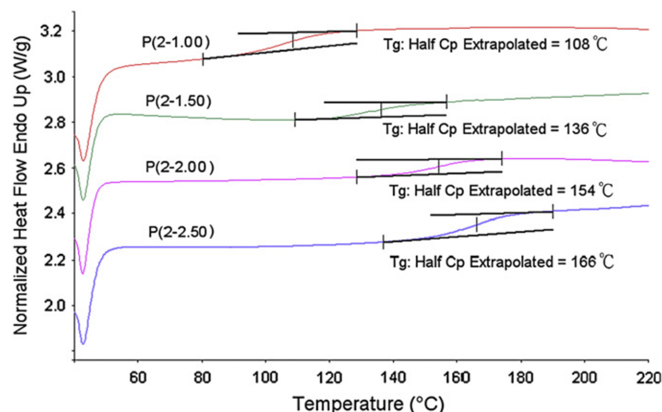

Fig. 6. DSC thermograms of self-cured **P(2)**.

2.2.1. Characterization

Differential scanning calorimetry (DSC) was performed with a Perkin–Elmer DSC 7 in nitrogen atmosphere at a heating rate of 20 °C/min. Tg was taken as the midpoint of the heat capacity transition between the upper and lower points of deviation from the extrapolated liquids and glass lines. Thermal gravimetric analysis (TGA) was performed with a Seiko EXSTAR 600 at a heating rate of 20 °C/min in nitrogen atmosphere. Dynamic mechanical analysis (DMA) was performed with a Perkin–Elmer Pyris Diamond DMA with a sample size of 5.0 × 1.0 × 0.2 cm. The storage modulus E' and tan δ were determined as the sample was subjected to the temperature scan mode at a programmed heating rate of 5 °C/min at a frequency of 1 Hz. The test was performed by bending mode with an amplitude of 5 μm. Coefficient of thermal expansion (CTE) was measured with a Seiko TMA/SS6100 at a heating rate of 5 °C/min. Epoxy equivalent weight (EEW) of the epoxy resins were determined by the $HClO_4$/potentiometric titration method. NMR measurements were performed using a Varian Inova 600 NMR in DMSO-d_6, and the chemical shift was calibrated by setting the chemical shift of DMSO-d_6 as 2.49 ppm. The UL-94 vertical test was performed according to the testing procedure of FMVSS 302/ZSO 3975 with a test specimen bar of 127 mm in length, 12.7 mm in width and about 1.27 mm in thickness. In the test, the polymer specimen is subjected to two 10-s ignitions. After the first ignition, the flame is removed and the time for the polymer to self-extinguish (t_1) is recorded. Cotton ignition would be noted if polymer dripping occurs during the test. After cooling, the second ignition is performed on the same sample and the self-extinguishing time (t_2) and dripping characteristics are recorded. Five specimens were performed. If the average t_1 plus t_2 is less than 10 s without any dripping, the polymer is considered to be

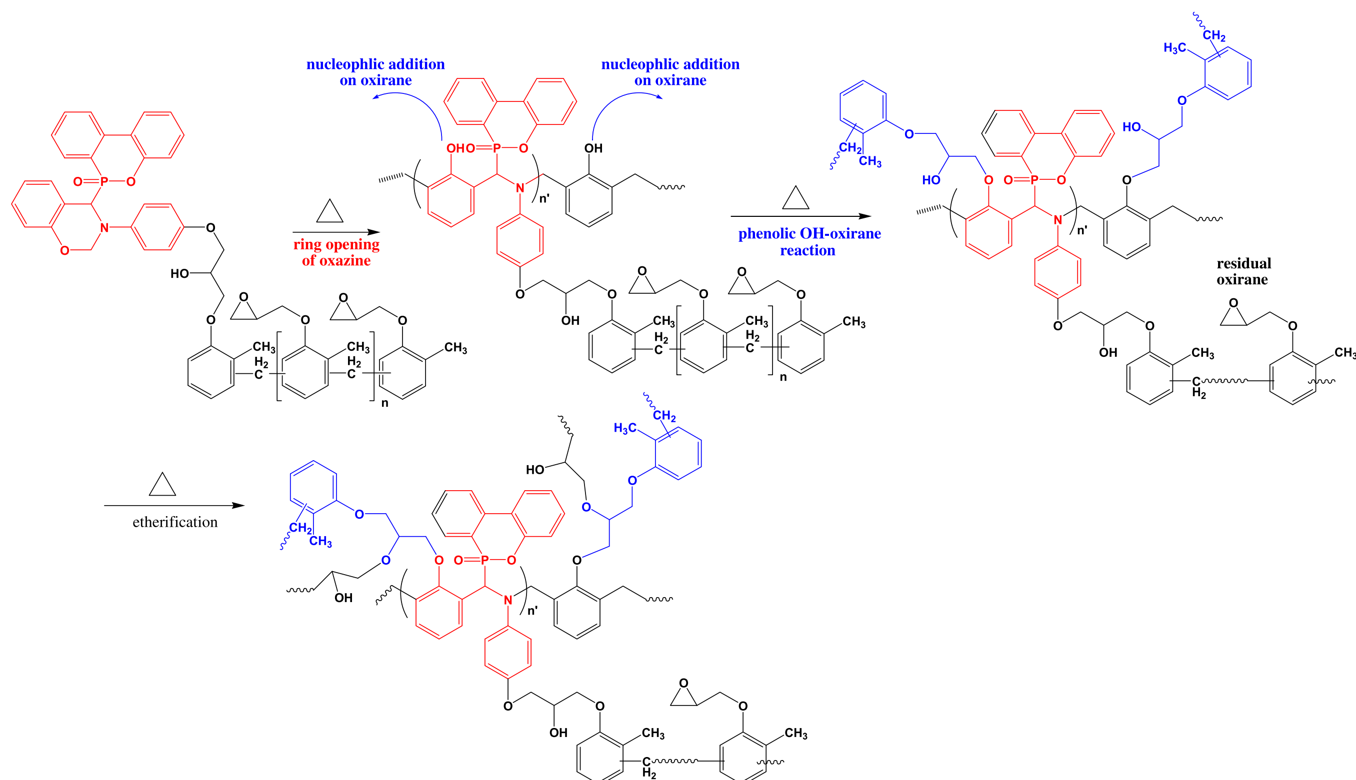

Scheme 3. Proposed polymerization mechanism of self-cured P(**2**).

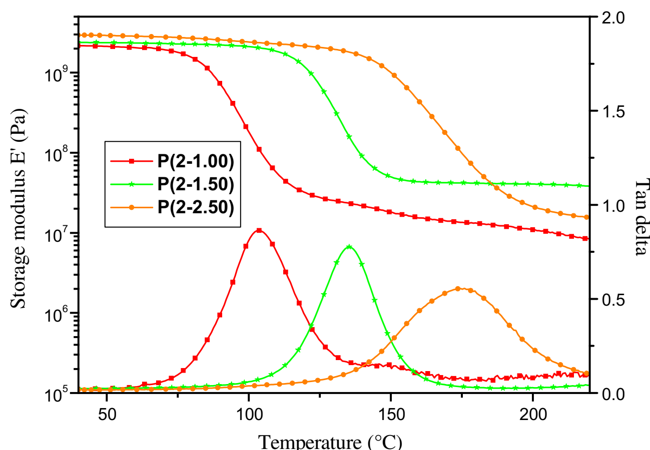

Fig. 7. DMA curves of self-cured **P(2)**.

a V-0 material. If t_1 plus t_2 is in the range of 10–30 s without any dripping, the polymer is considered to be a V-1 material. IR Spectra were obtained by Perkin–Elmer RX1 infrared spectrophotometer in KBr powder form. High resolution mass spectra were obtained by a Finnigan/Thermo Quest MAT 95XL mass spectrometer.

3. Result and discussion

3.1. Synthesis and characterization of (1)

In our previous paper, benzoxazine **(1)** was prepared by a three-pot procedure [27]. The first step is the condensation of 2-hydroxybenzaldehyde with 4-aminophenol, forming an intermediate (1a) with an imine linkage. The second step is the addition of DOPO on the imine linkage, resulting in an intermediate (1b) with a secondary amine linkage. The last step is the ring closure condensation of (1b), leading to benzoxazine (1) with a p-hydroxyphenyl linkage. However, the three-pot procedures are time consuming and the overall yield is not very high. Herein, we reported a one-pot procedure, in which intermediates (1a) and 1(b) were not isolated, to simplify the procedure and increase the yield. The reaction can be conducted with quantitative yield in various solvents such as methanol, ethanol and acetone, with yield values of 91%, 88%, and 84%, respectively, which is much higher than that (60%) prepared by the three-pot procedures [27]. In the ^{1}H-NMR spectrum, the characteristic oxazine peaks at around 5.20–5.50 ppm supported the structure of benzoxazine. In the ^{13}C-NMR spectrum, the characteristic peaks of N–CH_2–O and N–CH–ph at 57.20–58.59 and 76.65–77.06 ppm, respectively, also support the structure of benzoxazine. According to spectroscopic data, (1) prepared by this one-pot procedure has the same structure as that prepared by the three-pot procedure.

3.2. Synthesis and characterization of (2)

A series of epoxy resins (2) with various phosphorus contents were prepared by the nucleophilic addition of phenolic OH of **(1)** on the oxirane of CNE. This reaction was monitored by EEW titration and ^{1}H-NMR spectra. Generally, a catalyst with lone pairs such as triphenylphosphine or imidazole is required to initiate the nucleophilic addition. In this case, no external catalyst is required because of the lone pairs of nitrogen in **(1)**; that is, this is a self-catalytic reaction. Fig. 1 shows the plot of EEW versus reaction time at various reaction temperatures for **(2–1.5)**. As in Fig. 1, the reaction time required to reach the theoretical EEW (309 g/eq) is about 0.5 h, 2.5 h, 6 h and 8 h for 170 °C, 160 °C, 150 °C and 140 °C, respectively. Fig. 2 shows the ^{1}H-NMR trace of **(2–1.5)** at 140 °C for various reaction times. The signals of phenolic OH and the aromatic hydrogens (H^a and H^b) reduced after 4 h, and disappeared after 8 h, indicating that the reaction was complete 8 h. This result is consistent with that of EEW titration. Besides, the appearance of a signal of a secondary alcohol (H^e) and small peaks of Ar–H at 7.2–8.4 ppm support the nucleophilic addition. Fig. 3 shows the ^{1}H-NMR trace of **(2–1.5)** at 170 °C for various reaction times. The signals of phenolic OH and the aromatic hydrogens (H^a and H^b) reduced quickly after 20 min, and disappeared completely after 30 min. This result is also consistent with that of EEW titration. In addition, the characteristic peaks of oxazine still remain after 40 min, indicating no ring opening of oxazine linkage at 170 °C within 40 min. However, to avoid the gelation resulting from the ring opening of oxazine linkage, reaction at temperature higher than 170 °C is not recommended. Fig. 4 shows the plot of conversion (based on the integration area of H^a–H^b versus Ar–H in the NMR spectra) versus reaction time at various temperatures for **(2–1.5)**. The trend is consistent with that of EEW titration.

3.3. DSC thermograms

Fig. 5 shows the DSC thermograms of CNE and **(2)**. There is no exothermic peak during heating scan for neat CNE, while an obvious exothermic peak was observed for **(2)**. The enthalpy of exothermic peak increases with the content of oxazine linkage. It was thought that the ring opening of oxazine should be responsible for the exothermic peak. In addition, after the ring opening of oxazine linkage, a phenolic OH was formed, which can initiate the ring opening of oxirane [28–30]. Therefore, the nucleophilic addition of resulting phenolic OH on the oxirane may also be responsible for the exothermic peak. The etherification of secondary hydroxyl group on the oxirane that generally occurred in epoxy-rich systems at higher curing temperature might also be responsible for the exothermic

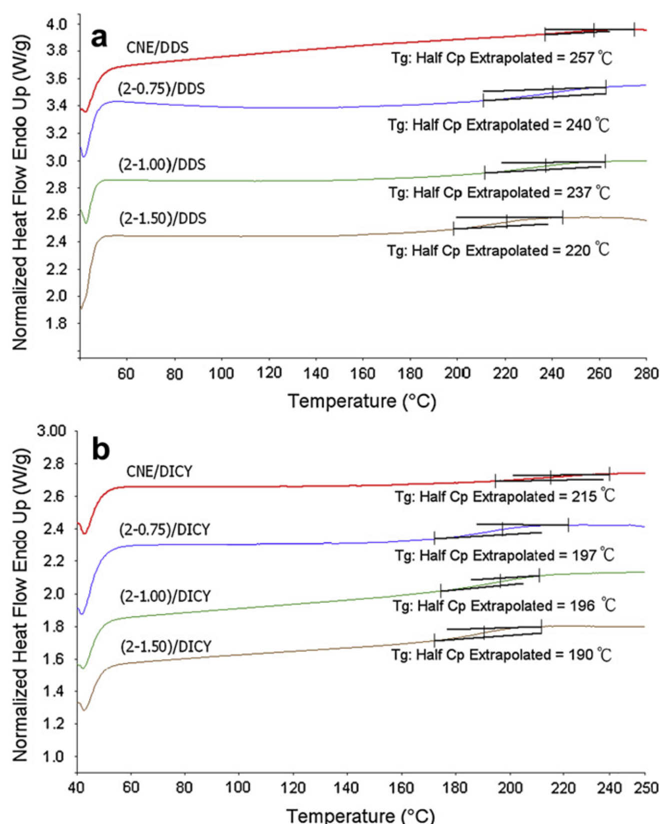

Fig. 8. DSC thermograms of curing agent-cured **P(2)**.

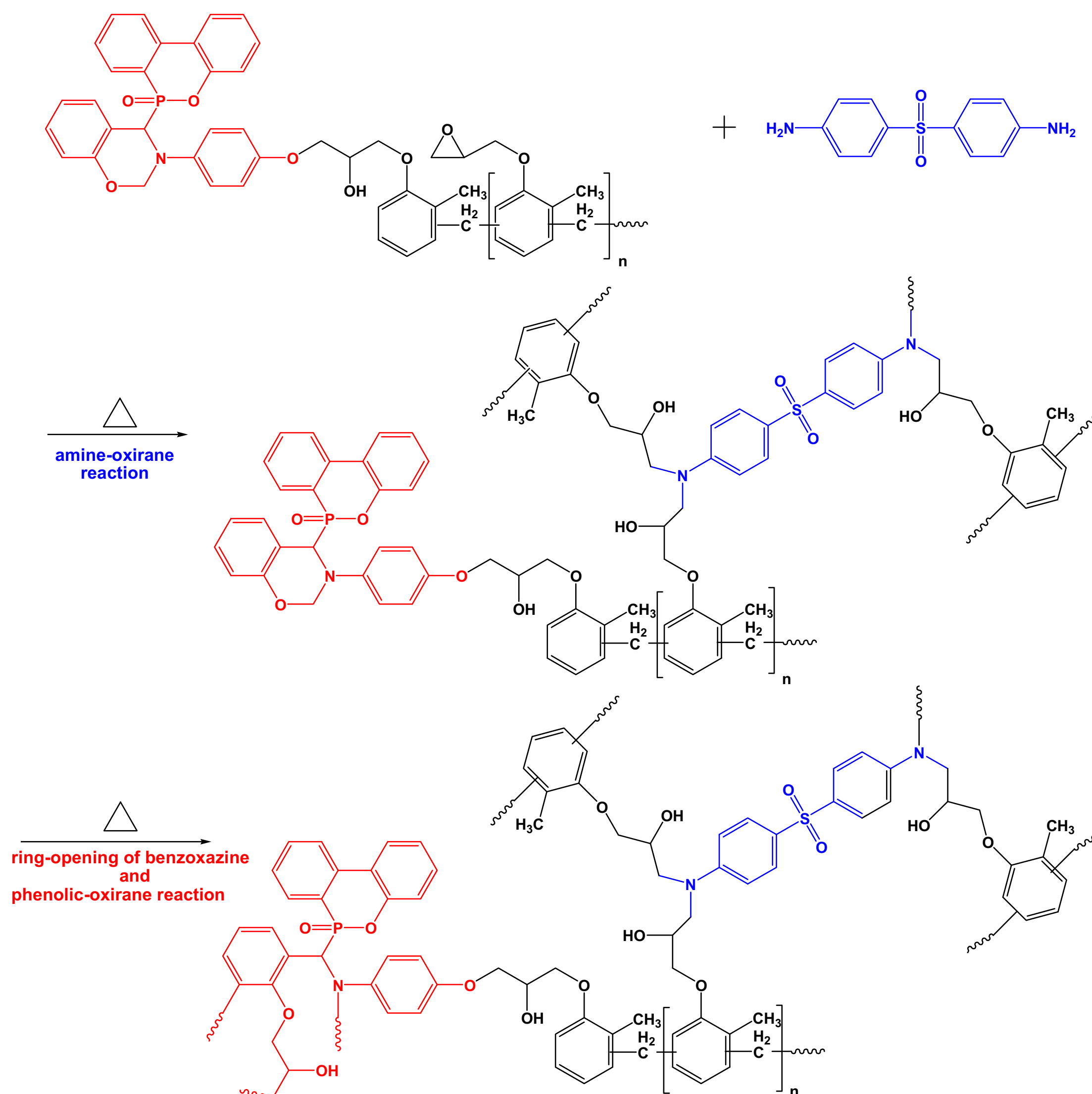

Scheme 4. Proposed polymerization mechanism of DDS-cured P(**2**).

peak. According to IR analyses (not shown), a ether shoulder at 1038 cm^{-1} was observed for self-cured P(2–2.0) after curing at temperature higher than 220 °C, supporting the etherification. Scheme 3 presented the proposed polymerization mechanism of self-cured P(**2**). The first stage was the ring opening of benzoxazine, the second stage was the nucleophilic addition of phenolic OH on oxirane, and the third stagewas the etherification of secondary hydroxyl group on the oxirane.

4. Properties of thermosets

4.1. Properties of self-cured (2) series

Since **(2)** showed the curing characteristic in the DSC scans (Fig. 5), they were then self-cured (without any curing agents) at 200 °C for 2 h. Fig. 6 shows the DSC thermograms of self-cured **(2)**. Tg ranges from 108 to 166 °C, and increases with the content of oxazine linkage. The ratio of phenolic OH/oxirane is 0.08, 0.14, 0.22, and 0.33 for self-cured P(**2–1.0**), P(**2–1.5**), P(**2–2.0**), and P(**2–2.5**), respectively. The lower Tg of **P(2–1.0)** can be explained by the insufficient ratio of phenolic OH/oxirane (0.08 in this case), which leads to low crosslinking density. In addition, the residual oxirane become a chain end, and thus increases the free volume of thermosets, and consequently leads to lower Tg. In contrast, the higher phenolic OH/oxirane ratio (0.33 in this case) in **P(2–2.5)** results in higher crosslinking density and smaller free volume, and leads to higher Tg. This speculation can be confirmed by the DMA curves of

Table 1
Thermal properties of **(2)/DDS** and **(2)/DICY** thermoset.

Thermoset ID	E′ (GPa)[a]	Tg (°C)[b]	Tg (°C)[c]	Tg (°C)[d]	CTE[e]	Td (°C)[f]	Char yield[h]
CNE/DDS	3.4	263	256	257	71	390	25
(2–0.75)/DDS	3.2	245	240	216	58	372	32
(2–1.00)/DDS	2.5	242	237	212	58	364	33
(2–1.50)/DDS	1.9	228	220	208	59	363	37
CNE/DICY	2.1	229	213	213	58	361	21
(2–0.75)/DICY	2.7	201	197	196	55	353	25
(2–1.00)/DICY	3.0	197	196	184	57	349	26
(2–1.50)/DICY	3.0	196	190	178	56	331	25

[a] modulus at 50 °C,, measured by DMA.
[b] (°C)peak of tan δ, measured by DMA.
[c] (°C)measured by DSC.
[d] (°C) measured by TMA.
[e] (ppm/°C) Coefficient of thermal expansion before Tg.
[f] (°C) 5% decomposition temperature in nitrogen atmosphere.
[h] (wt%) residual weight percentage at 800 °C in nitrogen atmosphere.

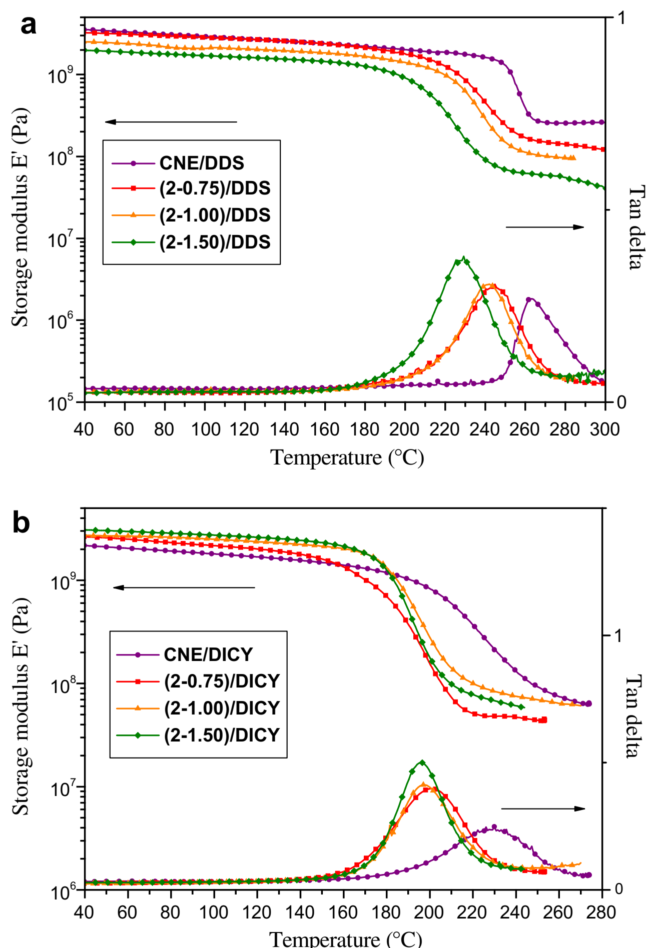

Fig. 9. DMA curves of (a) **(2)/DDS** and (b) **(2)/DICY** thermosets.

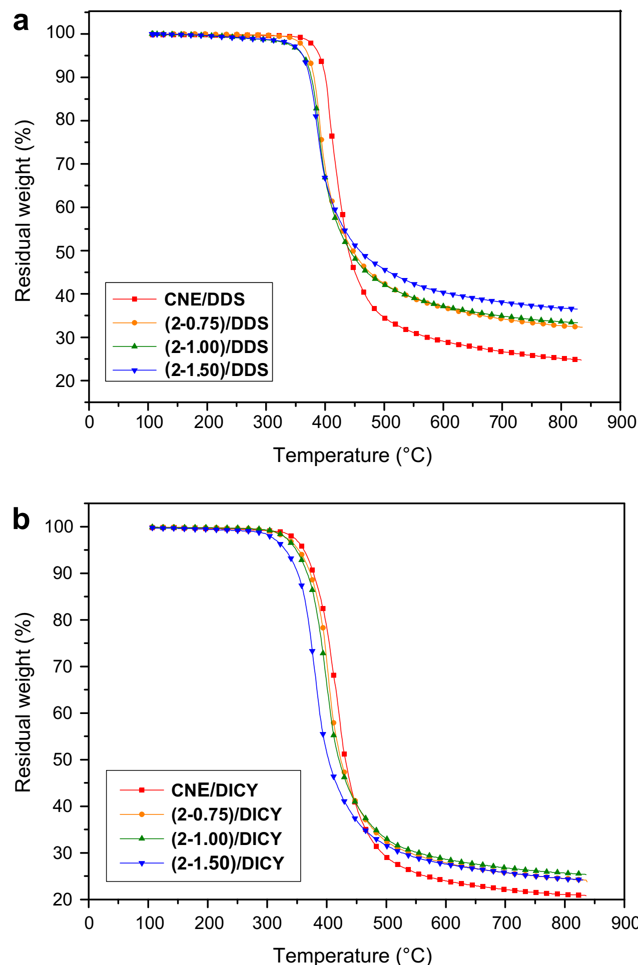

Fig. 10. TGA thermograms of (a) **(2)/DDS**, and (b) **(2)/DICY** thermosets in nitrogen atmosphere.

self-cured **P(2)** (Fig. 7). As shown in Fig. 7, the heights of tan (delta) are in the order of P(**2–2.5**) < P(**2–1.5**) < P(**2–1.0**). According to the principle of DMA, lower height of tan (delta) is associated with higher crosslinking density. Thus, from DMA data, the crosslinking density of self-cured **P(2)** are in the order P(**2–2.5**) > P(**2–1.5**) > P(**2–1.0**), increasing with the phenolic OH/oxirane ratio.

4.2. Properties of curing agent-cured (**2**) series

To enhance the crosslinking density, the equivalent ratio of active hydrogen-to-oxirane should be equal to one. Thus, two common epoxy curing agents for copper clad laminate, DDS and DICY, were incorporated to cure (**2**). Fig. 8 shows the DSC thermograms of **(2)**/DDS and **(2)**/DICY thermosets. As in Fig. 8, Tg increases significantly from 108 °C for self-cured P(**2–1.0**) to 237 °C for (**2–1.0**)/DDS thermoset, and from 136 °C for self-cured P(**2–1.5**) to 220 °C for (**2–1.5**)/DDS thermoset. The curing agent, which makes the ratio of active hydrogen-to-oxirane equal to one and thus enhances the crosslinking density, should be responsible for the improved Tg. According to IR and DSC analyses (not shown), the proposed polymerization mechanism of DDS-cured P(**2**) was shown in Scheme 4. The first stage is the nucleophilic addition of amine on oxirane, and the second stage is the ring opening of oxazine. The ring opening of oxazine linkage at the second stage maintained the crosslinking density, so high-Tg thermosets can be achieved. As listed in Table 1, higher Tg phenomenon was also observed for DICY-cured system. For example, Tg increases significantly from 108 °C for self-cured P(**2–1.0**) to 196 °C for (**2–1.0**)/DICY thermoset, and from 136 °C for self-cured P(**2–1.5**) to 190 °C for (**2–1.5**)/DICY thermoset. The high-Tg characteristics of thermosets can further be confirmed by DMA measurement (Fig. 9). For **(2)**/DDS system, a thermoset with Tg as high as 245 °C can be obtained when an UL-94 V-0 rating was achieved (will be discussed later). To our knowledge, this is the highest Tg for epoxy resins suitable for printed circuit board. As to the dimensional stability, TMA data shows that the CTEs are in the range of 55–59 ppm/°C for both **(2)**/DDS and **(2)**/DICY systems, indicating good dimensional

Table 2
Flame-retardant test of **(2)/DDS** and **(2)/DICY** thermoset.

Thermoset ID	P (wt%)[a]	N (wt%)[b]	t_1 (s)[c]	t_2 (s)[d]	UL-94 Rating
CNE/DDS	0	2.67	>60	–	Burning
(2–0.75)/DDS	0.61	2.35	6.5	2.6	V-0
(2–1.00)/DDS	0.82	2.34	3.9	2.5	V-0
(2–1.50)/DDS	1.26	2.32	3.1	1.9	V-0
CNE/DICY	0	4.36	>60	–	burning
(2–0.75)/DICY	0.72	3.54	7.5	2.7	V-1
(2–1.00)/DICY	0.95	3.46	5.2	1.2	V-0
(2–1.50)/DICY	1.43	3.3	1.4	0.9	V-0

[a] Phosphorus content.
[b] Nitrogen content.
[c] First average burning time.
[d] Second average burning time.

stability. Fig. 10 show the TGA thermograms of (a) **(2)/DDS**, and (b) **(2)/DICY** thermosets. The 5 wt% decomposition temperatures are in the range of 363–372 °C for (**2**)/DDS system and 331–353 °C for (**2**)/DICY system, demonstrating moderate to high thermal stability when compared with other phosphorus-containing epoxy thermosets [31]. In addition, the char yields were improved for the phosphorus-containing thermosets. Table 2 listed the flame-retardant test of (2)/DDS and (2)/DICY thermosets. An UL-94 V-0 rating can be achieved with an overall phosphorus content as low as 0.61 wt% for (**2**)/DDS thermoset, which is extremely low for epoxy thermosets. However, for the DOPO-modified epoxy/DDS thermoset [12], an overall phosphorus content of 1.69 wt% is required for a V-0 rating. The excellent flame retardancy must be due to the higher crosslinking density and the flame-retardant nature of oxazine linkage. Besides, the nitrogen–phosphorus synergistic effect [32,33] might also contribute to the excellent flame retardancy of this system. The high-Tg characteristic makes **(2)** attractive for high Tg copper clad laminates, which are much valuable than the low Tg one.

5. Conclusions

A one-pot procedure of preparing benzoxazines **(1)** with a p-hydroxyphenyl linkage was revealed. Based on **(1)**, a series of (**1**)-modified CNE, (**2**), were successfully prepared by nucleophilic addition of **(1)** and CNE. According to EEW titration and NMR analysis, the nucleophilic addition can carry out without external catalyst such as imidazole or triphenylphosphine. It is thought that the lone pairs of nitrogen in **(1)** catalyzed the reaction. According to DSC and DMA measurement, **(2)** can be self-cured, but the Tgs of self-cured P(**2**) are not very high. The insufficient phenolic OH-to-oxirane ratio explained the low Tg phenomenon. However, Tg improved significantly after curing with curing agent. For example, Tg increases significantly from 108 °C for self-cured P(**2**–**1.0**) to 237 °C for (**2**–**1.0**)/DDS thermoset, and from 136 °C for self-cured P(**2**–**1.5**) to 220 °C for (**2**–**1.5**)/DDS thermoset. The curing agent, which makes the ratio of active hydrogen-to-oxirane equal to one and thus enhances the crosslinking density, should be responsible for the improved Tg. For the **(2)**/DDS thermoset, an overall phosphorus content as low as 0.61 wt% is sufficient for a UL-94 V-0 rating, and the corresponding Tg is as high as 245 °C. To our knowledge, this is the highest Tg for epoxy resins suitable for printed circuit board. The ring opening of oxazine linkage at the later curing stage, which maintained the crosslinking density, explained the high Tg value. The flame-retardant nature of oxazine linkage and nitrogen–phosphorus synergistic effect might be responsible for the low phosphorus content required for flame retardancy. Based on these promising resins, manufacturing of flame-retardant copper clad laminates is in progress.

Acknowledgements

The authors thank the National Science Council of the Republic of China for financial support. Partially sponsorship by the Green Chemistry Project (NCHU), as funded by the Ministry of Education is also gratefully acknowledged.

References

[1] Komori K, Kashihara K, Ogasawara K, Nozue A, Okada S. (Matsushita Electric Works, Ltd). U.S. Patent 6403690, 2002.
[2] Nakamura Y, Asano T, Ogasawara KIN. (Matsushita Electric Works, Ltd). U.S. Patent 6645630, 2003.
[3] Takahashi T, Uchida T, Fujioka AN. JP Kokai 10-30017 1998; CA 128:154846.
[4] Takahashi T, Uchida T, Fujioka A. JP Kokai 10-30016 1998; CA 128:154845.
[5] Yoshizawa M, Kobayashi N. JP Kokai 10-152545 1998; CA 129:41816.
[6] Lin CH, Wu CY, Wang CS. J Appl Polym Sci 2000;78:228.
[7] Alcon MJ, Ribera G, Galia M, Cadiz V. J Polym Sci Part A Polym Chem 2005;43:3510.
[8] Wang CS, Berman JR, Walker LL, Mendoza A. J Appl Polym Sci 1991;43:1315.
[9] Stephens EB, Tour JM. Macromolecules 1993;26:2420.
[10] Stephens EB, Kinsey KE, Davis JF, Tour JM. Macromolecules 1993;26:3519.
[11] Morgan AB, Tour JM. Macromolecules 1998;31:2857.
[12] Lin CH, Wang CS. Polymer 2001;42:1869.
[13] Allcock HR, Hartle TJ, Taylor JP, Sunderland NJ. Macromolecules 2001;34:3896.
[14] Allcock HR, Powell ES, Maher AE, Berda EB. Macromolecules 2004;37:5824.
[15] Perez RM, Sandler JKW, Altstät V, Hoffmann T, Pospiech D, Ciesielski M, et al. Polymer 2007;48:778.
[16] Liu WC, Varley RJ, Simon GP. Polymer 2007;48:2345.
[17] Wang WS, Chen HS, Wu YW, Tsai TY, Chen-Yang YW. Polymer 2008;49:2826.
[18] Ryu BY, Moon S, Kosif I, Ranganathan T, Farris RJ, Emrick T. Polymer 2009;50:767.
[19] Ellzey KA, Ranganathan T, Zilberman J, Coughlin EB, Farris RJ, Emrick T. Macromolecules 2006;39:3553.
[20] Ranganathan T, Zilberman J, Farris RJ, Coughlin EB, Emrick T. Macromolecules 2006;39:5974.
[21] Copper clad laminates based on the resins and their derivatives are produced by Nan Ya Plastics Corporation.
[22] Zhang XH, Liu F, Chen S, Qi GR. J Appl Polym Sci 2007;106:2391.
[23] Schäfer A, Seibold S, Lohstroh W, Walter O, Döring M. J Appl Polym Sci 2007;105:685.
[24] Schäfer A, Seibold S, Walter O, Döring M. Polym Deg Stab 2008;93:557.
[25] Seibold S, Schäfer A, Lohstroh W, Walter O, Döring M. J Appl Polym Sci 2008;108:264.
[26] Odian George, editor. Principle of polymerization. 3rd ed., 108. Wiley-Interscience; 1991.
[27] Lin CH, Lin HT, Chang SL, Hwang HJ, Hu YM, Taso YR, et al. Polymer 2009;50:2264.
[28] Ishida H, Rodriguez Y. J Appl Polym Sci 1995;58:1751.
[29] Espinosa MA, Cadiz V, Galia M. J Polym Sci Part A Polym Chem 2004;42:279.
[30] Espinosa MA, Cádiz V, Galiá M. J Appl Polym Sci 2003;90:470.
[31] Liu YL, Hsiu GH, Lee RH, Chiu YS. J Appl Polym Sci 1997;63:895.
[32] Wu CS, Liu YL, Chiu YS. Polymer 2002;43:4277.
[33] Zhu SW, Shi WF. Polym Deg Stab 2002;75:543.